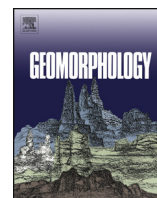




Contents lists available at ScienceDirect

Geomorphology

journal homepage: www.elsevier.com/locate/geomorph

Late Holocene chronology and geomorphic development of fluvial–tidal floodplains in the upper reaches of the lower Columbia River Valley, Washington and Oregon, USA

Curt D. Peterson^{a,*}, Michael C. Roberts^b, Sandy Vanderburgh^c, Rick Minor^d, David Percy^a

^a Portland State University, 1721 SW Broadway, Portland, OR 97207-0751, United States

^b Simon Fraser University, 8888 University Drive, Burnaby, BC V5A1S6, Canada

^c Lethbridge College, Lethbridge, Alberta T1K1H6, Canada

^d Heritage Research Associates, Inc., 1997 Garden Ave., Eugene, OR 97403, United States

ARTICLE INFO

Article history:

Received 5 March 2013

Received in revised form 16 July 2013

Accepted 29 July 2013

Available online xxx

Keywords:

Fluvial–tidal

Floodplains

Late Holocene

Sea level rise

Depositional rates

ABSTRACT

The upper reaches of the lower Columbia River Valley (125 km in length) comprise an alluvial system that is transitional between fluvial and fluvial–tidal dominance. Sinuous channels separate elongate islands (1–8 km in length) and floodplains (0.5–12.7 km in total width). Thirty-six floodplain overbank deposits are analyzed for age and depth, which demonstrate an average sedimentation rate of 1.6 m ka⁻¹ during the last 5–6 ka. Older core records confirm that long-term depositional rates are controlled by relative sea level rise. Rising floodplain groundwater surfaces, which followed relative sea level rise (~1.25 m ka⁻¹), submerged isolated floodplain depressions. Low sedimentation rates in the isolated depressions (0.6–1.1 m ka⁻¹) maintained large ellipsoidal bullseye lakes (7–22 km² in area) dating back to 3.5–4.0 ka. Increases in the widths of the floodplains and bullseye lakes are associated with broadening of the incised valley (4–13 km width) in the Portland Basin. Dated basal overbank deposits (0.5–5.0 ka in age) and their separation distances establish channel migration rates of 0.3–1.9 km ka⁻¹. Shallow burial rates relative to rapid channel migration rates resulted in reworking of late Holocene floodplains (50–75% erosion) since 5 ka in the upper reaches of the lower Columbia River Valley.

© 2013 Elsevier B.V. All rights reserved.

1. Introduction

In this paper we use floodplain topography and dated sediment cores to describe how late Holocene floodplains developed in the lower Columbia River Valley (LCRV) in Washington and Oregon (Fig. 1).

The floodplains that developed under the unusual conditions of high sediment supply (Sherwood and Creager, 1990), net sea level rise, and restricted channel migrations in the narrow antecedent valley (Peterson et al., 2011) are not easily classified in terms proposed for some other fluvial–tidal systems (Nanson and Croke, 1992; Allen and Posamentier, 1993; Dalrymple et al., 1994). The late Holocene wetlands, lakes, and discharge channels in the LCRV floodplains provided important hunting, fishing, and gathering resources for Native Americans (Saleeby, 1983; Minor et al., 1994; Darby, 1996; Butler, 2004; O'Rourke, 2005). However, no archaeological sites in upper reaches of the LCRV are reported with ages >3.5 ka (Minor et al., 2010).

During historic time the construction of dikes, drainage ditches, floodgates and landfills altered many of the floodplain habitats in the LCRV (Sherwood et al., 1990; Simenstad et al., 1990). Results from this study show that maintenance of some long-lived water bodies, now

identified as bullseye lakes, in the altered floodplains will require raising groundwater surface levels to higher elevations near the floodplain lakes. Restoring floodplain wetland habitats and small discharge channels will require removing floodplain dikes and flood gates that have isolated floodplain interiors from seasonal flooding since the early 1900s.

Floodplain surface elevations, established by LiDAR, and subsurface deposits, dated by tephrochronology and AMS radiocarbon analysis, provide constraints on late Holocene sedimentation rates and channel migration rates. Floodplain surface areas, elevations and sedimentation rates are largely related to incised valley widths in the narrow antecedent valley. Long-term floodplain deposition and preservation, respectively, in the upper reaches of the LCRV are related to burial from submergence and lateral channel migration rates in the fluvial tidal system. The origins of floodplain features in the LCRV should have broader relevance to the uppermost reaches of other antecedent fluvial–tidal systems that developed in forearc settings under conditions of high sediment supply, net sea-level rise, and narrow incised-valley widths.

2. Background and previous work

The upper reaches of the LCRV are located in an incised valley into which the Willamette, Lewis, and Cowlitz Rivers flow (Fig. 1). These reaches of the LCRV range from to 1 to 13 km in width, with the greatest widths occurring in the forearc Portland basin. Mean annual discharge

* Corresponding author.

E-mail addresses: peterson@pdx.edu (C.D. Peterson), mroberts@sfu.ca (M.C. Roberts), sandy.vanderburgh@lethbridgecollege.ca (S. Vanderburgh), RickMinorHRA@aol.com (R. Minor), percy@pdx.edu (D. Percy).

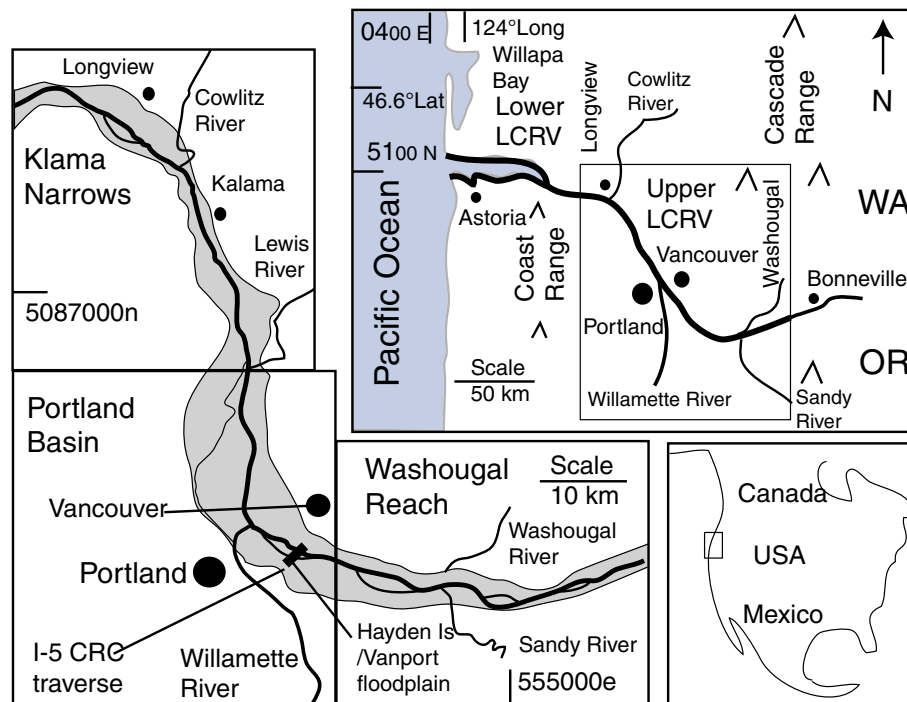


Fig. 1. Location of the lower Columbia River valley (LCRV) is antecedent in the Cascade volcanic arc and the Coast Range. The LCRV crosses the Willamette and Cowlitz–Lewis forearc valleys that are located between the Cascade and Coast Ranges. Three sections of the upper reaches are geographically defined on the basis of incised river valley widths including (1) the Washougal reach, (2) the Portland basin, and (3) the Kalama narrows.

of the Columbia River is $6700 \text{ m}^3 \text{ s}^{-1}$ (Sherwood and Creager, 1990). Maximum latest summer tidal range (September–October) in the upper reaches of the LCRV decreases from 2.1 m (Longview, WA) to 1.5 m (Vancouver, WA) to 0.2 m (Bonneville, WA) along a river kilometer distance of about 125 km. The upper tidal reaches of the LCRV, as defined here, occur upriver of Longview, WA. They are all fresh water. The upper tidal reaches are located from about 100 to 225 km distance upriver of the river mouth at the Pacific Ocean. Early historic flood heights of the Columbia River in the Portland basin reached 10.6 m above the low river levels (Gates, 1994). Prolonged spring floods followed snowmelt in the northeastern tributary basins, prior to the many historic impoundments of most of the Columbia's tributaries (Simenstad et al., 1990; Jay et al., 2011).

Transgressive depositional filling of the submerged valley during early to middle Holocene time (11–5 ka) buried the incised valley floor under 20–50 m of fluvial sand and mud (Fig. 1) (Peterson et al., 2011). In late Holocene time the lower rates of net sea level rise ($\sim 1.25 \text{ m}$ per thousand years or m ka^{-1}) allowed the abundant sediment supply ($10\text{--}15 \text{ million t y}^{-1}$) (Sherwood and Creager, 1990) to outpace increasing basin accommodation space (Peterson et al., 2012a). Suspended load and bedload were largely bypassed to the lower estuarine reaches and/or the ocean beaches (Baker et al., 2010; Peterson et al., 2010; Twichell et al., 2010). However, migrating channels in the upper reaches of the fluvial–tidal system permitted temporary stabilization of floodplains and the accumulations of overbank deposits, which are the subjects of this article.

3. Methods

LiDAR data coverage provides 1/9 arc sec bareground digital elevation models (DEM nominal $\pm 0.1 \text{ m}$ elevation) for modern floodplain surfaces of the upper reaches of the LCRV (PugetSoundLidar, 2013). The LiDAR DEMs were used with GIS orthorectified satellite images to (i) tie core site elevations to the regional NAVD88 elevation datum (Fig. 2A–C) (Table 1) and (ii) provide supplemental surface elevation

data on the basis of nonbiased point grid spacing of 1.0 or 2.0 km. The elevation data that are presented in this paper are relative to the NAVD88 datum, which is equivalent to the lowest river–tidal level or about 1 m below mean sea level (MSL) in the study area.

Late Holocene floodplain deposits were auger cored or gouge cored to 3–10 m subsurface depth (Fig. 2A, B, and C). Deeper boreholes were sampled with rotary sonic drilling to at least 30 m depth in the Hayden Island and Vanport I–5 CRC traverse, between Portland, OR and Vancouver, WA (Peterson et al., 2011). Continuous cores were photographed and logged to 1 cm scale. Core sediment samples were analyzed for mud, sand, plant macrofossil content, and distinctive waterlain tephra layers (Peterson et al., 2012b). Sand size fractions were analyzed with an AM/CAN Stratigraphic calibrated grain size card as follows: vFL (62–88 μ), vFU (88–125 μ), fL (125–177 μ), fU (177–250 μ), mL (250–350 μ), mU (350–500 μ), cL (500–710 μ), and cU (710–1000 μ).

Deposit dating was completed using tephrochronology and AMS radiocarbon dating. Key tephra marker beds in the LCRV that are dated at 0.5, 1.3, 2.5–3.0, 3.5–4.0, and 7.7 ka are described in detail elsewhere (Peterson et al., 2012b). Small twigs were preferentially selected for AMS dating to reduce errors from (i) young carbon in descending roots or (ii) old carbon in large wood fragments that could have been reworked from previous deposits. Radiocarbon ages are presented in cal. YBP at the two-sigma ($2\text{-}\sigma$) analytical error (Beta Analytic Inc., Miami, FL). Dated overbank deposits are used to establish floodplain sedimentation rates and channel migration rates.

4. Results

4.1. Washougal reach

The uppermost reaches of the antecedent LCRV (1–1.5 km valley width) lack any significant floodplain development. Narrow floodplains (0.5–2.2 km total floodplain width) do occur downriver in the slightly widening Washougal reach (2–4 km valley width) (Fig. 2A). Core site

elevations in the Washougal reach indicate that the floodplains range from 5.5 to 9.0 m in height above low river level (Table 1). Preserved muddy overbank deposits and prehistoric archaeological sites in the

Table 1
Core site positions and surface elevations in floodplains.

Core site	UTMe (m)	UTMn (m)	Elev. (m)	Core site	UTMe (m)	UTMn (m)	Elev. (m)
CRR11	555355	5044315	6.9	CRSR1	547561	5045144	6.9
CRSR3	547240	5045462	5.7	CRMC1	541349	5045824	5.5
MU84	541000	5045000	8.0	MU106	541085	5045005	8.0
CRGI2	541781	5046227	5.5	CRGI1	539417	5046120	8.0
CL118	538900	5048200	8.0	CRL11	533861	5048617	7.0
BH1	524952	5051015	4.0	BH2	524584	5050297	4.0
BH3	524918	5049944	2.4	BH4	524566	5050049	3.5
CRXP2	524246	5050125	2.3	BH7c	524676	5049513	2.7
TB5	524540	5049450	1.5	BH8d	524686	5049221	1.5
CRS11	514103	5055630	12.8	CRS12	510930	5058440	14.0
CRS13	512697	5065061	5.7	CRS16	514572	5057880	3.0
CRS15	517491	5064236	4.0	CRS14	517571	5064243	6.0
CRB11/2	518112	5072725	5.0	CRB13	517686	5075422	6.0
CRVL7	521154	5060271	3.5	CRVL6	520047	5057556	3.6
CRVL9	520295	5059810	8.7	CRVL8	520500	5060700	4.9
CRVL3	518534	5059272	5.5	CRVL2	518511	5059297	4.0
45CL31	523400	5057500	4.0	CRWL1	516934	5081315	4.3
CRWL3	515616	5084978	4.5	CRDL1	513678	5088670	4.7
CRDI2	513198	5087343	5.6	CRRF1	500092	5105873	2.5
CRRF2	500341	5106651	3.9	CRLV1	497345	5111119	2.1
CRLV2	500603	5110088	1.4				

Core positions are in meters (m) 10 N UTM coordinates, easting and northing. Core site elevations are in meters (m) NAVD88 taken from 1/9 arc sec LiDAR digital elevation models. Core site elevations are reported to 0.1 m, but nominal LiDAR accuracy (± 0.1 m) is reduced for core site elevations (assumed ± 0.25 m) because of uncertainty of 12 channel RT-GPS (2–5 m horizontal error). Site 45CL31(A) was reported by Wessen (1983), but could not be confirmed by these authors.

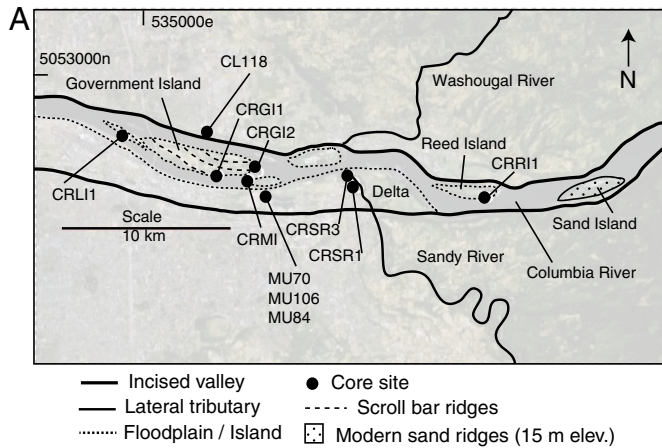
narrow floodplains yield relatively young ages of 0.5–3.4 ka (Fig. 3; Table 2).

4.2. Portland basin

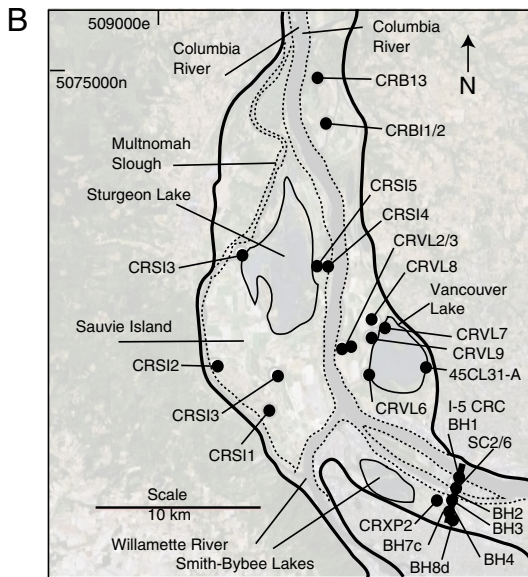
The substantially wider Portland Basin (4–13 km valley width) contains broad floodplains (2.7–12.7 km total floodplain width) (Fig. 2B). With the exception of the southwest end of Sauvie Island, representative core site elevations in the widest floodplains range from 1.5 to 8.7 m in height above the low river level (Table 1). The Vanport floodplain occurs just upriver of the Willamette River confluence. The narrowest width of the Vanport floodplain (1.7 km) at the I–5 CRC traverse in the Portland basin is associated with the oldest known continuous sequence of preserved floodplain deposits in the LCRV (0–9 ka in age) (Table 2) (Peterson et al., 2011). Nonrooted mud, rooted mud, and discontinuous interbeds of nonrooted muddy sand were found in the late Holocene deposits of the Vanport floodplain (0–5 ka) (Fig. 4).

The widest floodplains (10–12.7 km total width) in the study area occur just downriver of the Willamette River confluence (Fig. 2B). These floodplains are characterized by truncated scroll bar sequences that record channel avulsions and migrations, dated from 0.5 to 4.0 ka (Fig. 5). The highest elevations occur at the southwest end of Sauvie Island where sand ridges reach 12.8 m elevation at core site CRS11 and 14.0 m elevation at core site CRS12. Silt deposits (1.5 m thick) top the thick sand sequences at both of the high ridge core sites. The highest sand ridges exceed the heights of pre-dam or earliest-historic river floods (10.6 m elevation NAVD88) in the Portland Basin (Gates, 1994).

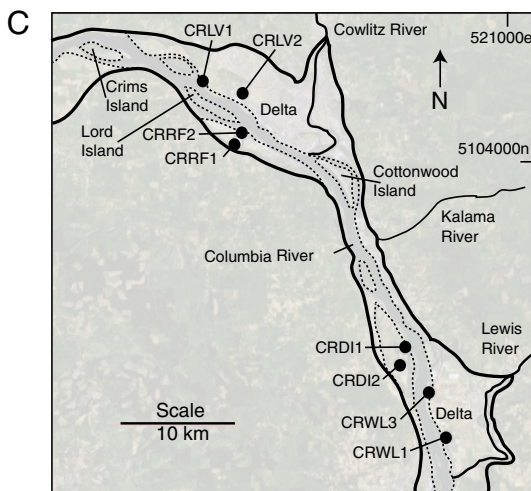
Fig. 2. (A) Map of Washougal Reach floodplain morphology. Numbered core sites or trench sites (solid circles) are shown in the mid-channel islands and floodplains (dotted lines). Sites at CL118, MU84, and MU106 are dated archaeological sites (Minor et al., 2010). Government Island retains prominent scroll bars. Sand Island contains sand dune ridges (15–20 m elevation). (B) Map of Portland Basin floodplain morphology. Numbered core sites or borehole sites (solid circles) are shown in the mid-channel islands and floodplains (dotted lines). (C) Map of Kalama Narrows floodplain morphology. Numbered core sites (solid circles) are shown in the mid-channel islands and floodplains (dotted lines). Interior sites in the lateral tributary deltas of the Cowlitz and Lewis Rivers were avoided in this study because of field evidence of floodplain reworking by delta distributary channels.



— Incised valley ● Core site
— Lateral tributary - - - - Scroll bar ridges
..... Floodplain / Island □ Modern sand ridges (15 m elev.)



— Incised valley ● Core site
..... Floodplain / Island



— Incised valley ● Core site
— Lateral tributary
..... Floodplain / Island

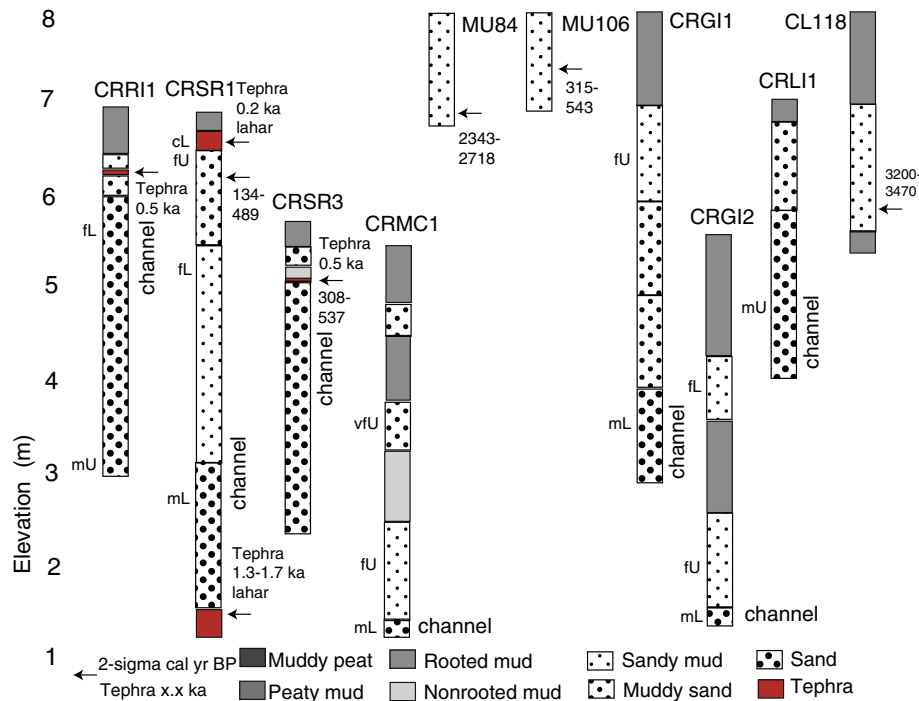


Fig. 3. Core logs and dates from narrow floodplains and mid-channel islands in the Washougal reach. Mud overbank deposits are very thin (<0.5 m thickness) in CRR11 (Reed Island), CRSR1 and CRSR3 (Sandy River Delta), and CRL11 (Lemon Island) suggesting very young ages for those channel-reworked settings. Core site positions and elevations are shown in Fig. 2A and Table 1.

The interior of the Sauvie Island floodplain (Fig. 2B) contains the large Sturgeon Lake (22 km² in surface area), which is dated to at least 3.5 ka in core site CRSI3 (Fig. 5). The shallow lake is bounded by a scroll bar ridge and swale sequence dated at 3 ka in core site CRSI6. The eastern side of the Sauvie Island floodplain is dated at 0.5 ka in core site CRSI4.

The Vancouver floodplain contains the large Vancouver Lake (11 km² in surface area), dated to about 4.0 ka in core site CRVL7 (Fig. 6) by radiocarbon and prominent tephra layer (MSH set-Y) (Fig. 7). Vancouver Lake is bounded to the west by a large scroll bar ridge dated to at least 2.8 ka in core site CRVL9. The western side of the Vancouver floodplain is dated to about 0.5 ka in core site CRVL3.

4.3. Kalama narrows

The incised valley narrows downriver in the Kalama narrows (1.5–4.5 km wide), with corresponding local decreases in most floodplain widths (0.5–2.5 km total width) (Fig. 2C). Exceptions occur at the Cowlitz and Lewis River deltas where delta floodplains reach about 4 km in width. Core site elevations in floodplains in the Kalama narrows range from 1.4 to 5.6 m in height above the low river level (Table 1). Measured floodplain ages in the Kalama Narrows range from 1.3 to 3.9 ka (Fig. 8).

In this study only the main channel margins of the Sandy, Lewis, and Cowlitz River deltas (Fig. 2A, B, and C) were investigated for subsurface lithology and age. Those lower floodplain elevations were directly influenced by the Columbia River. Core logs from the lower floodplains of the deltas demonstrate flood silts of at least 3 m thickness that extend back to at least 1.3 ka in CRWL3 and 2.9 ka in CRLV2 (Fig. 8).

Remnant distributary channel and lobe features in the Cowlitz and Lewis River deltas (Fig. 2C) attest to prolonged delta progradation into the central incised valley. A similar finding is reported from deeper cores taken in the Sandy River delta in the Washougal reach (Fig. 2A) (Rapp, 2005). The latest Holocene progradations of the small tributary deltas of the Sandy, Lewis, and Cowlitz Rivers have displaced the main Columbia River channel to the opposite sides of the incised valley,

thereby locally influencing main channel alignments in the narrow antecedent valley.

The large Sauvie Island floodplain (Fig. 2B) occurs just below the confluence of the very large Willamette River tributary (Fig. 1). Morphologically, the Sauvie Island floodplain does not resemble a tributary delta, but its presence does appear to have stabilized the major channels of the Columbia River in the center of the incised valley after 3.0 ka (Fig. 5).

5. Discussion

5.1. Average floodplain elevations

A general decrease in averaged core site elevations occurs from the narrow Washougal reach (7.0 m elevation; sample number = 10) to the wide Portland basin (4.3 m elevation; sample number = 26) (Table 1; Fig. 2A and B). Excluding artificial landfills the modern floodplain surface elevations were largely stabilized during (i early historic time (early 1900s) by extensive dikes, drainage ditches, and flood gates and (ii later historic time (middle 1900s) by reduced floods from more than 100 large impoundments in tributaries (Sherwood et al., 1990; Simenstad et al., 1990).

The apparent decreases in floodplain elevations at core sites in the widening incised valley of the Portland basin reflect (i decreasing sedimentation rates with increasing distance from the major channels, as discussed below, and probably (ii decreasing peak flood heights in the wider valley. Floodplain core site elevations rise slightly in the narrowing reaches of the Kalama narrows (Fig. 2C; Table 1). However, farther downriver, in the estuarine reaches of the LCRV (0–100 km from the river mouth) (Fig. 1), the widening valley contains relatively few floodplains and those few floodplains rarely exceed 3–4 m in elevation.

A survey of floodplain elevations in the upper reaches of the LCRV utilizing bareground LiDAR (Pugetsoundlidar, 2013) was conducted to supplement the limited core site elevation data shown in Table 1. Because of the occurrence of extensive dikes and road lifts in the

Table 2
Radiocarbon and tephra dates from late Holocene floodplains.

Core site	Depth (m)	Material	Eruption event	Convention YBP	Calibrated Cal. YBP	Beta #
CRR1	0.7	Tephra	MSH set-W			
CRSR1	0.2	Tephra	Old Maid			
CRSR1	0.6	Wood		250 ± 70	134–489	B76446
CRSR1	5.3	Tephra	Timberline			
CRSR3	0.6	Tephra	MSH set-W			
CRSR3	0.7	Wood		410 ± 70	308–537	B67448
MU84	1.1	Char		2420 ± 70	2343–2718	B46485
MU106	0.6	Char		430 ± 60	315–543	B241088
CL118	2.1	Char		3130 ± 70	3200–3470	B158461
RC7	15.0	Tephra	MSH set-Y			
BH1	1.8	Wood		310 ± 40	290–490	B276961
SC15	16.5	Tephra	MSH set-Y			
BH2	1.5	Tephra	SH/A1.3 ka			
BH2	10.6	Tephra	MSH set-Y			
BH2	11.3	Wood		4100 ± 40	4450–4820	B271643
BH3	0.3	Tephra	MSH set-W			
BH3	1.5	Tephra	SH/A1.3 ka			
BH3	7.5	Tephra	MSH set-Y			
BH3	7.5	Wood		3460 ± 40	3630–3840	B271644
BH3	13.5	Wood		6150 ± 50	6900–7170	B271645
BH3	19.0	Tephra	MAZ set-O			
BH3	27.5	Wood		7900 ± 50	8590–8980	B271647
BH4	2.4	Tephra	SH/A1.3 ka			
BH4	8.5	Tephra	MSH set-Y			
BH4	22.0	Tephra	MAZ set-O			
BH4/SC8	31.0	Wood		8020 ± 40	8760–9020	B288782
CRXP2	0.3	Tephra	MSH set-W			
CRXP2	2.4	Tephra	SH/A1.3 ka			
CRXP2	4.8	Tephra	MSH set-P			
BH7c	2.5	Wood		2120 ± 40	1990–2160	B276965
BH7c	6.1	Tephra	MSH set-P			
BH7c	7.1	Wood		4290 ± 40	4830–4880	B276966
BH7c	8.8	Tephra	MSH set-Y			
BH7c	17.0	Tephra	MAZ set-O			
BH7c	26.0	Wood		8030 ± 50	8730–9020	B276967
TB5	8.3	Tephra	MSH set-Y			
BH8d	0.7	Tephra	SH/A1.3 ka			
BH8d	6.9	Tephra	MSH set-Y			
BH8d	8.3	Wood		5290 ± 50	5930–6200	B276968
BH8d	20	Tephra	MAZ set-O			
BH8d	24.5	Wood		7930 ± 50	8600–8990	B276970
BH8	8.0	Tephra	MSH set-Y			
CRS13	4.4	Wood		3200 ± 30	3380–3470	B326995
CRS13	5.8		MSH set-Y			
CRS16	2.5	Char		2850 ± 95	2767–3222	GaK5570
CRS15	1.5	Tephra	SH/A1.3 ka			
CRS14	2.9	Wood		410 ± 30	450–510	B326994
CRVL7	4.5	Peat		3710 ± 40	3960–4150	B327001
CRVL7	4.7	Tephra	MSH set-Y			
CRVL9	4.0	Wood		2670 ± 50	2740–2860	B326993
CRVL8	5.7	Peat		4070 ± 50	4420–4810	B327002
CRVL2	1.6	Wood		600 ± 30	650–540	B326997
45CL31-A	0.5	Char		3510 ± 100	3511–4084	B3556
CRBI1/2	3.6	Wood		1410 ± 30	1290–1350	B326996
CRBI1/2	3.7	Tephra	SH/A1.3 ka			
CRWL3	2.8	Tephra	SH/A1.3 ka			
CRDI1	1.9	Wood		1480 ± 30	1310–1410	B326998
CRDI2	2.0	Tephra	SH/A1.3 ka			
CRLV2	1.8	Peat		2450 ± 30	2360–2710	B304399
CRLV2	1.9	Tephra	MSH set-P			
CRLV2	1.9	Peat		2790 ± 30	2800–2960	B304400
CRRF1	5.0	Tephra	MSY set-Y			
CRRF1	5.5	Wood		3710 ± 30	3930–4150	B326999

Notes: Depth is below floodplain surface level, does not include artificial fill. Fill depth in MU70 is not known. Possible truncation depth in 45CL31-A is not known.

Wood: predominantly twigs and small detrital wood fragments (wood), charcoal (char), felted roots/leaves or peaty (peat).

Tephra: predominantly ash size material, except for large lapilli (1 cm) in CRDI sites and lahar in CRSR1 (Peterson et al., 2012b).

Tephra dates: Old Maid (A.D. 1781), MSH set-W (A.D. 1480), SH/A1.3 ka (1260–1360 YBP), Timberline (1330–1740 YBP), MSH set-P (2500–3000 YBP), MSH set-Y (3500–4000 YBP), MAZ set-O (7700 YBP) (Peterson et al., 2012b).

Radiocarbon dates (B) are from Beta Analytic Inc., Miami, Florida, as shown with conventional (1-σ analytical error) and calibrated (2-σ analytical error).

GaK date is from Gakushuin University, Tokyo, Japan, obtained from adjacent archaeological site 35MU9 (Pettigrew, 1981).

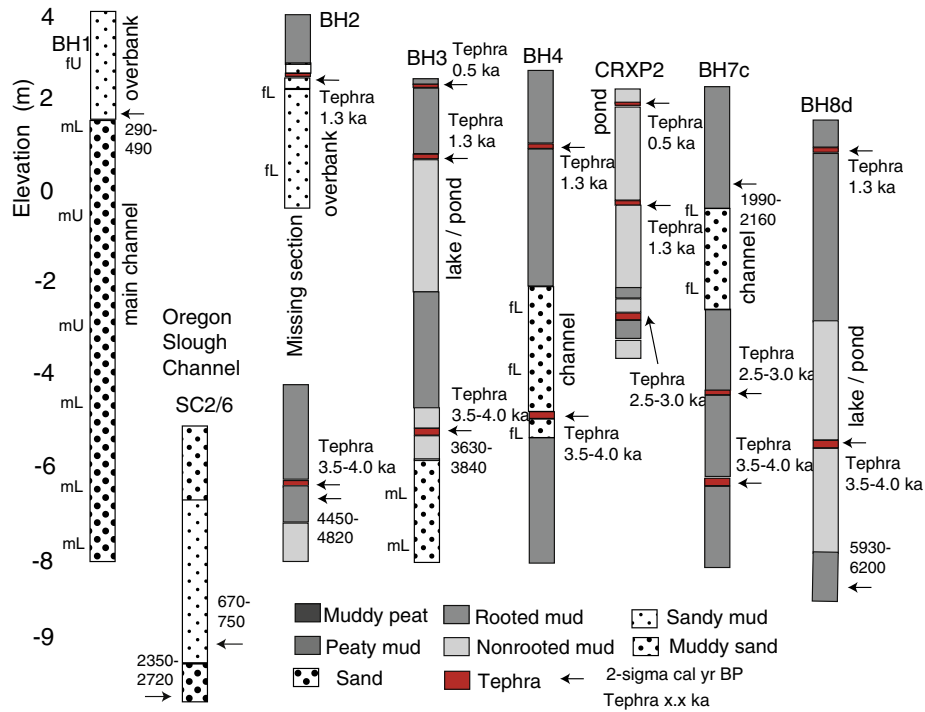


Fig. 4. Core logs and dates from Hayden Island (BH1) and the Vanport floodplain. Small discharge channels are interspersed between lakes and vegetated overbank settings (0–6 ka in age) in the low Vanport floodplain (historic surface 2–4 m elevation). Radiocarbon and tephrochronology data are presented in Table 2. Core site locations are shown in Fig. 2B.

floodplains, we used a grid method of selecting initial nonbiased point elevations and then adjusted some points ± 50 –100 m distance to avoid dikes, road lifts, and artificial landfills. Floodplain elevation points were collected at 1.0-km grid spacing in the narrow Washougal reach

and Kalama narrows and at 2.0-km grid spacing in the wider Portland basin (Table 3). Floodplain elevations were not collected in the Sandy River, Lewis River, and Cowlitz River deltas, where the incised valley is very locally widened and the delta distributary channels have reworked

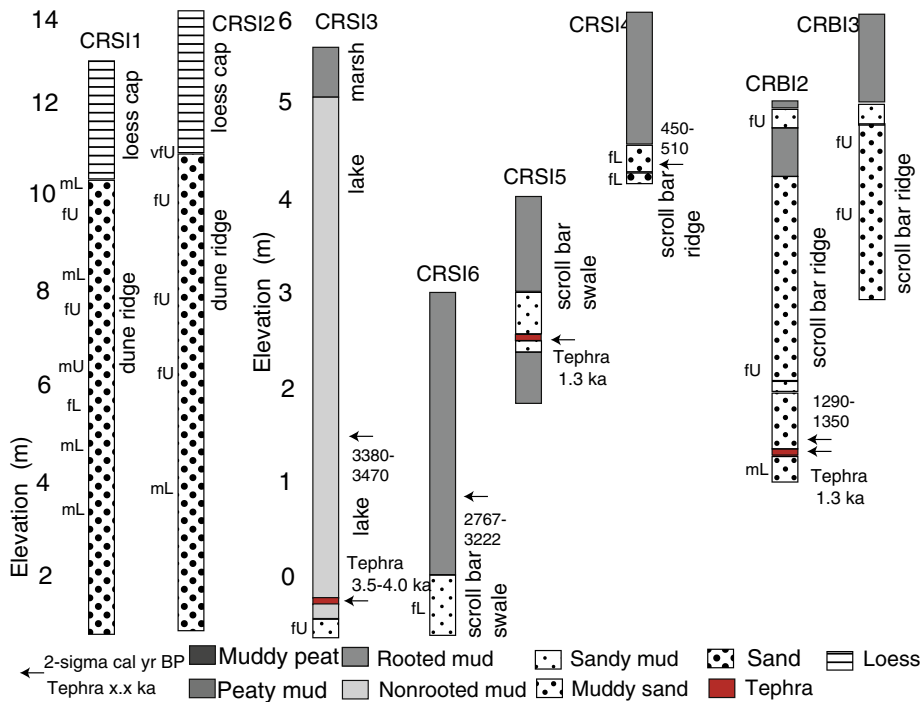


Fig. 5. Core logs and dates from the Sauvie Island and Bachelor Island floodplains. Anomalous high ridges are located in the southwest end of Sauvie Island between core sites CRSI1 and CRSI2. Thick deposits of fine sand, which are capped by silt loess (~1.5 m thick), occur in the high ridges. The shallow but large Sturgeon Lake (22 km² in surface area) contains nonrooted mud (lake facies), which dates back to at least 3.5 ka at core site CRSI3. A marsh (peaty mud) layer above the lake mud is assumed to represent historic marsh progradation under conditions of decreasing lake levels. Core site locations are shown in Fig. 2B.

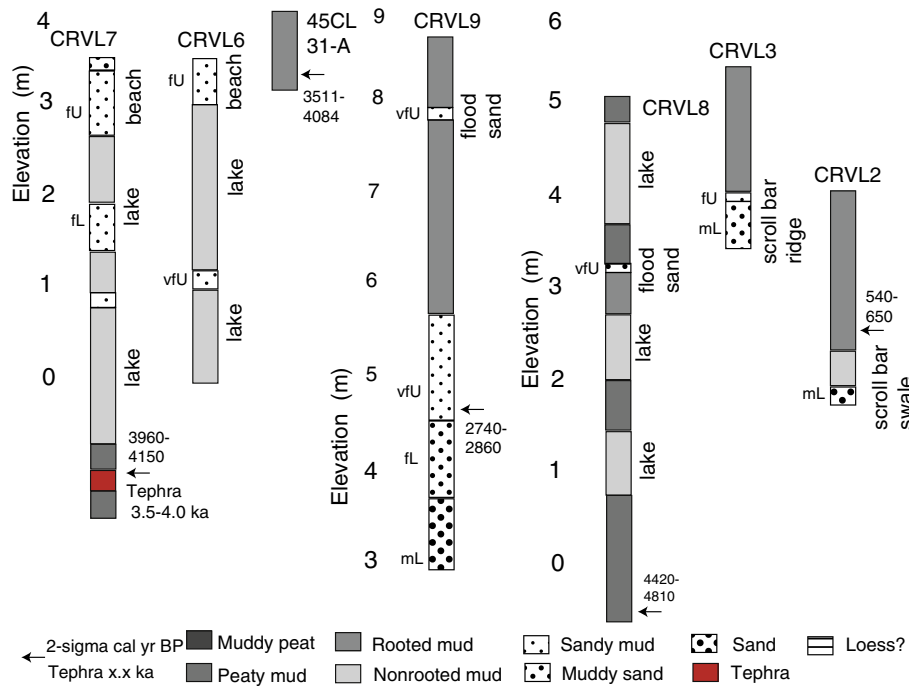


Fig. 6. Core logs and dates from the Vancouver floodplains. The large Vancouver Lake (11 km² in area) dates back to about 4 ka at core site CRVL7. A shallow cultural site (45CL31-A) on the east side of Vancouver Lake is dated by charcoal with fire cracked rock (FCR) at 3.5–4.0 ka (Wessen, 1983). Rooted beach deposits above lake level in CRVL7 and CRVL6 are partly due to artificial shoreline modifications, but sedges growing in the thin sand deposits denote lowering lake levels in historic time, relative to the nonrooted lake deposits in prehistoric time. The historic beach sand deposits are not included in estimates of prehistoric lake sedimentation rates. Distinct flood sand layers are rare (1 event since 4.5 ka) in the Shillapoo Pond core site (CRVL8). Shillapoo pond is a remnant of the larger Shillapoo Lake that existed prior to diking and draining of the Vancouver floodplain (USGS, 1905). Core site locations are shown in Fig. 2B.

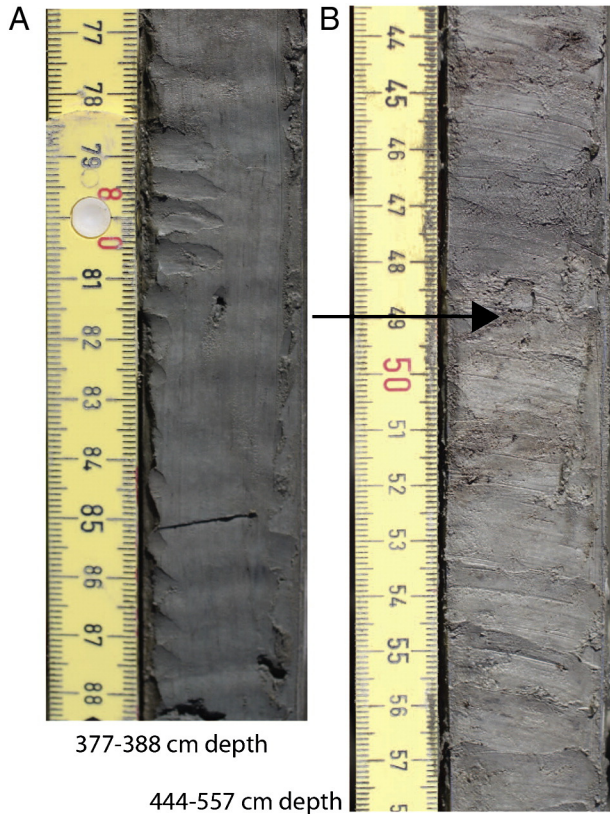


Fig. 7. Photos of Vancouver Lake core CRVL7 sections including (A) nonrooted lake mud at 377–388 cm depth and (B) rooted mud above tephra at 444–557 cm depth. Tephra (top at arrow) is from the Mount St. Helens set-Y eruption (3500–4000 YBP) (Table 2). The complete core log for CRVL7 is shown in Fig. 6.

the delta floodplains. Ground elevations in the shallow Sturgeon and Vancouver Lakes were estimated to be 3.5 and 2.5 NAVD88, respectively.

Totals of 28, 45, and 16 gridded elevation points were collected, respectively, in the Washougal reach (2.9-km average valley width), Portland basin (4.2-km average valley width), and Kalama narrows (2.2-km average valley width) (Table 3). Averaged floodplain elevations are 7.1 ± 1.7 m for the Washougal reach (585 km² floodplain area), 4.2 ± 1.7 m for the Portland basin (1590 km² floodplain area), and 4.8 ± 1.3 m for the Kalama narrows (259 km² floodplain area). The gridded point elevation data demonstrates trends of decreasing floodplain elevation with increasing valley width and increasing floodplain surface area between the Washougal Reach and the Portland Basin. The Kalama Narrows host the least of the length-normalized floodplain areas (7 km²/km section length), but the averaged floodplain elevation remains at a modest height (~5 m elevation) in the narrow antecedent river reach.

5.2. Chronology of late Holocene floodplain development

Floodplain overbank deposits from the upper reaches of the LCRV were dated by radiocarbon and/or tephrochronology (Table 2). The dated deposits are plotted for depth below surface and age (Fig. 9). A modest positive correlation ($R^2 = 0.7$; sample number = 36) exists between sample depth and age. The least squares estimated trend line yields an average sedimentation rate of 1.6 m ka^{-1} for the late Holocene (0–6 ka) floodplain deposits. This average sedimentation rate is close to the rate of sea level rise ($\sim 1.25 \text{ m ka}^{-1}$) estimated for the late Holocene in the study area (Peterson et al., 2010).

5.3. Sedimentation rates in proximal versus distal floodplain settings

The modest correlation between sample depth and age (Fig. 9) reflects a significant variability in sedimentation rates between different

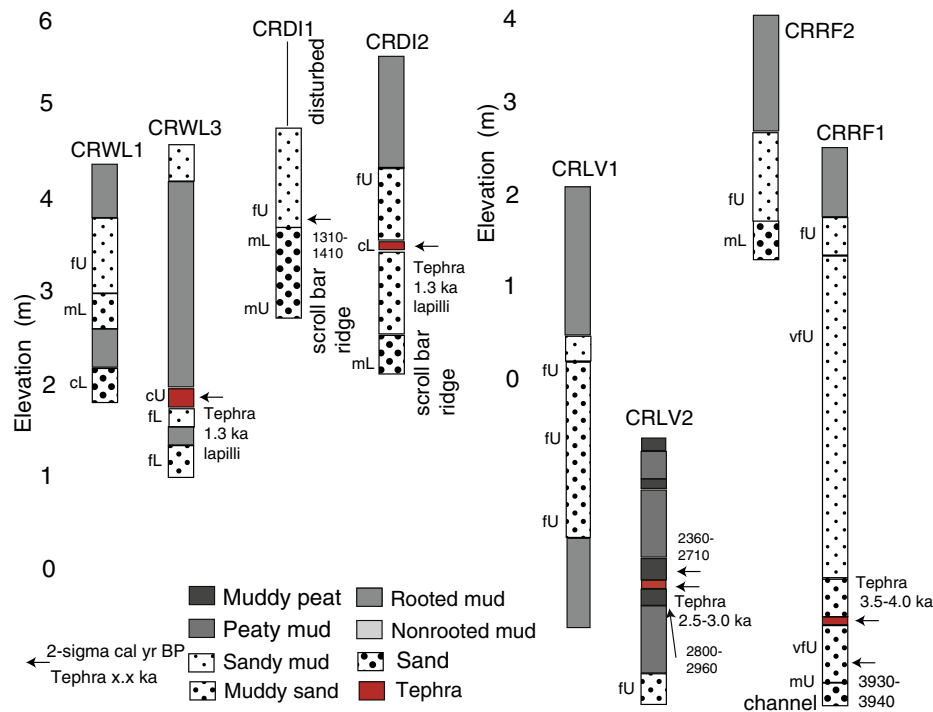


Fig. 8. Core logs from the Woodland (CRWL sites), Deer Island (CRDI sites), Longview (CRLV sites), and Rainier (CRRF) floodplains. The Woodland and Longview core sites are located in floodplains of lateral tributary deltas from the Lewis and Cowlitz Rivers. Core site locations are shown in Fig. 2C.

floodplain settings. To address this variability, some dated overbank deposits from cores sites in different types of floodplain settings are compared for measured sedimentation rates (Table 4).

Core site BH1 in Hayden Island is located at a distance of 250 m from the main Columbia River channel (Fig. 2B). Two Vanport floodplain sites, CRXP2 in Force Pond and BH3 in a low elevation wetland, are both located about 1500 m from the main Columbia River channel. A seven fold difference in sedimentation rates between the core sites in Hayden Island and the Vanport floodplain occurred during the last 500 years (Table 4), which demonstrates the importance of floodplain proximity to main channel overbank deposition in controlling short-term sedimentation rate. We speculate that this relation results from preferential settling of fine sand and silt fractions out of suspension near channel margins where floodwater turbulence decreases with distance away from major channels.

Sedimentation rates are compared between two vegetated wetland sites BH7c and CRRF1 of the same elevation (2.5–2.7 m NAVD88) and distance from a main channel (~1.5 km) but at widely separated sites, upriver and downriver, respectively, in the study area (Fig. 2A and C). The two sites are separated by about 70 km distance along the river valley. These two core sites yield about the same sedimentation rates

(1.4–1.5 m ka^{-1}) during the last 4–5 ka (Table 4), suggesting that suspended load sediment supply probably does not vary substantially downriver within the study area.

5.4. Low sedimentation rates in isolated lakes

Three core sites CRSI3, CRLV7 and CRLV8 from Sturgeon, Vancouver, and Shillapoo Lakes in the Portland basin (Fig. 2B) show significantly lower sedimentation rates of 0.7–1.1 m ka^{-1} than the averaged value of 1.6 m ka^{-1} during the last 3–4 ka (Table 4). These large lakes are currently separated from the major Columbia River channels by distance (2–4 km) and intervening scroll bar ridges (6–8 m NAVD88) (Figs. 6 and 7).

The distributions of floodplain sizes, sedimentation rates, and elevations in the upper reaches of the LCRV differ from generalized models of coastal alluvial systems that rely on river gradient, base profile, or base level to predict geomorphic trends (Blum and Törnquist, 2000). In this study, we find that a major influence on floodplain development is incised valley width. Increasing incised valley width generally decreases both floodplain surface elevations (Table 3) and overbank sedimentation rates (Table 4).

Table 3
Incised valley widths, floodplain surface areas, and elevations.

Section	Valley length (km)	Valley width (km)	Area (km ²)	Area/length (km ² /km)	Mean elev. (m)	Std. dev. elev. (±m)
Washougal	30	2.9	585	15	7.1	1.7
Portland	41	7.6	1590	39	4.2	1.7
Kalama	36	2.2	259	7	4.8	1.3

Notes: Section length (Length) is based on river km distance and does not include tributary deltas. Mean incised valley widths are averaged from across-valley widths between 9-m elevation contours, perpendicular to main channel orientations, taken at 2 km along valley spacing. Valley widths at Sandy, Lewis, and Cowlitz River deltas are not included in valley width averages. Floodplain surface area (Area) does not include tributary deltas or eolian dune ridges. Section length normalized floodplain area (Area/length) is in units of km²/km. Floodplain elevation is mean elevation of combined floodplains and mid-channel islands for each river section. Mean elevation (m NAVD88) is based on point elevations from representative grid spacing: 1-km grid centers in Washougal and Kalama sections and 2 km grid centers in the Portland section. Elevation point coordinates (UTM) for N = 28, N = 45, N = 16, respectively, for Washougal reach, Portland basin and Kalama narrows sections, and corresponding elevations (bareground LiDAR 1/9 arc sec) are provided in Supplement GridPointElev.

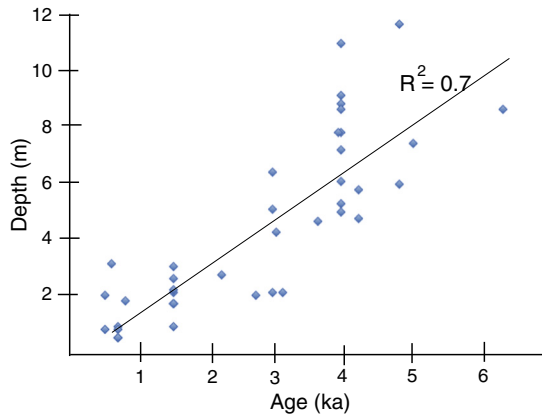


Fig. 9. Plot of overbank deposit thickness versus age for dated late Holocene deposits (samples = 36 in number) in the upper reaches of the LCRV. A least squares regression ($R^2 = 0.7$) yields a sedimentation rate trend of 1.6 m ka^{-1} for deposits dating back to 5–6 ka. Data are from Table 2.

5.5. Origins of elongate islands

Large elongate islands are developed upriver of the Willamette River confluence in the upper reaches of the LCRV (Fig. 2A and B). Hayden Island (8.5 km in length) is separated from the Vanport floodplain by a minor channel called Oregon slough (Fig. 10). Cores from boreholes drilled across Hayden Island and Oregon slough provide age control to

Table 4
Floodplain sedimentation rates.

Core site	Interval (ka)	Thickness (m)	Sedimentation rate (m ka^{-1})
<i>Hayden island</i>			
BH1	0–0.4	1.8	4.5
<i>Vanport floodplain</i>			
BH3	0–0.5*	0.3	0.6
BH3	0–1.3*	1.5	1.1
BH3	1.3*–4.0*	6.0	2.2
BH3	4.0*–7.7*	12.0	3.2
BH3	7.7*–8.8	9.5	8.6
BH4	0–1.3*	2.4	1.8
BH4	1.3*–4.0*	6.1	2.3
BH4	4.0*–7.7*	13.5	3.6
BH4	7.7*–8.8	5.5	5.0
BH7c	0–2.0	2.5	0.8
BH7c	1.3*–4.0*	7.2	2.7
BH7c	4.0*–7.7*	9.0	2.4
BH7c	7.7*–8.8	10.5	9.5
BH8d	0–1.3*	0.7	0.5
BH8d	1.3*–4.0*	6.2	2.3
BH8d	4.0–7.7*	13.0	3.5
BH8d	7.7*–8.8	10	9.1
<i>Bullseye lakes</i>			
CRS13	0–3.4	3.5	1.0
CRVL7	0–4.0	3.2	0.8
CRVL8	0–4.6	5.2	1.1
CRXP2	0–0.5*	0.3	0.6
<i>Vegetated floodplains</i>			
BH7c	0–4.8	7.1	1.5
CRRF1	0–4.0	5.5	1.4

Notes:
Tephra ages, as shown by (*), are based on eruption onset ages (Table 2) as follows: MSH set-W (0.5 ka), SH/A1.3 ka (1.3 ka), onset of MSH set-Y (4.0 ka), onset of Mazama set-O (7.7 ka) (Peterson et al., 2012b).
All other dates are from radiocarbon and they are taken at the mid-point of the 2-sigma calibration (ka).
See Table 2 for depth (thickness) of the dated late Holocene intervals.
Lake mud thickness in Sturgeon and Vancouver Lakes does not include historic marsh or beach sediments.
Sedimentation rate is interval thickness divided by interval age, yielding units of m ka^{-1} .

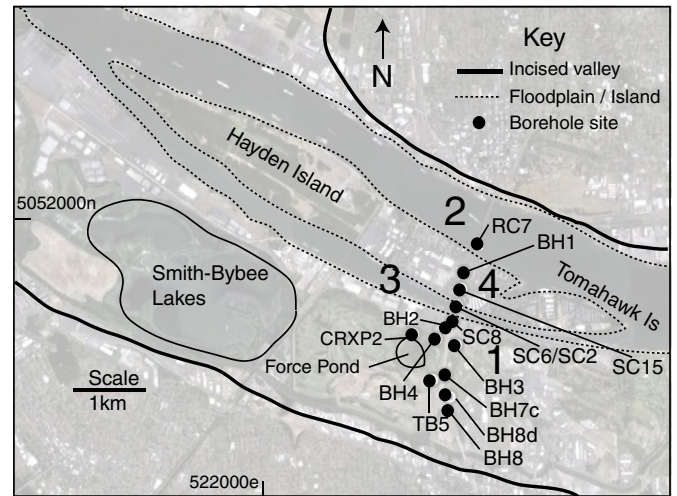


Fig. 10. Map of elongate Hayden Island and Vanport floodplain to the south, including Smith-Bybee Lakes (7 km² in total area) and the remnant Force Pond (0.3 km²). The sequence of Hayden Island formation is numbered (1 oldest to 4 youngest) as dated from borehole samples (solid circles) and associated core logs (Figs. 2B and 4). See text for explanation of numbered sequence.

establish the origins of the elongate island, as follows: (i) A major channel migrated south to truncate the northern edge of the Vanport floodplain at 4.0–2.5 ka, as dated in borehole SC6 in Oregon slough (Fig. 4; Table 2). (ii) The main channel bifurcated at the upriver end of the Hayden–Tomahawk Island complex and abandoned sandy overbank deposits in BH2 at 1.3 ka. It is not known what condition or event triggered the channel bifurcation at the upriver end of Hayden–Tomahawk Islands. (iii) The southern channel remained in place as Oregon slough deposited muddy sand in SC6 and SC2 at 0.6–0.7 ka, and the northern channel stabilized on the north side of an elongated sand shoal. (iv) The sand shoal began to vertically accrete to form Hayden Island from overbank muddy sand deposition by 0.3–0.5 ka at BH1.

Government Island (7.3 km in length) is located in the Washougal reach (Fig. 2A) where it demonstrates another form of elongate island separation from a lateral floodplain. Government Island retains scroll bar topography that cuts obliquely across the island. The oblique scroll bar topography predates the island’s separation from a larger floodplain. The remnant floodplain on the north side of the Columbia River at archaeological site CL118 is dated at 3200–3470 YBP (Fig. 3; Table 2). The age of the floodplain on the south side of the Columbia River, at archaeological site MU84 (Fig. 2A) is dated back to at least 2.4 ka (Minor et al., 2010). Major channel deposits in the west end of the Sandy River delta, upriver of Government Island, are reported to contain Timberline lahar sediments (1330–1740 YBP) (Table 2; Rapp, 2005). These lahar deposits were not observed at Government Island cutbank sites CRGR1 or CRGR2. The age of the Government Island scroll bar sequence is not known, but its preservation attests to the cutoff and abandonment origin of Government Island, probably after 2.4–3.4 ka.

Three smaller elongate Islands—Lemon Island (2.5 km length), Reed Island (3.3 km in length), and Sand Island (1.5 km in length) (Fig. 2A)—demonstrate longitudinal sand ridges that are aligned approximately parallel to the island shorelines. These islands formed in place and/or elongated downriver. Thin overbank flood silts in Lemon Island (0.2 m thick at site CRL11) (Fig. 3) and the young age of overbank deposits at Reed Island (~0.5 ka at site CRR11) demonstrate very recent origins for these mid-channel islands.

The origins of these small elongate islands correspond to major channel bends in the antecedent river valley (Fig. 2A) where diverged river flows permitted the sustained accumulation of sand bars. No other elongate or mid-channel islands are developed upriver of Reed and Sand Islands in the narrowing valley of the uppermost reaches of

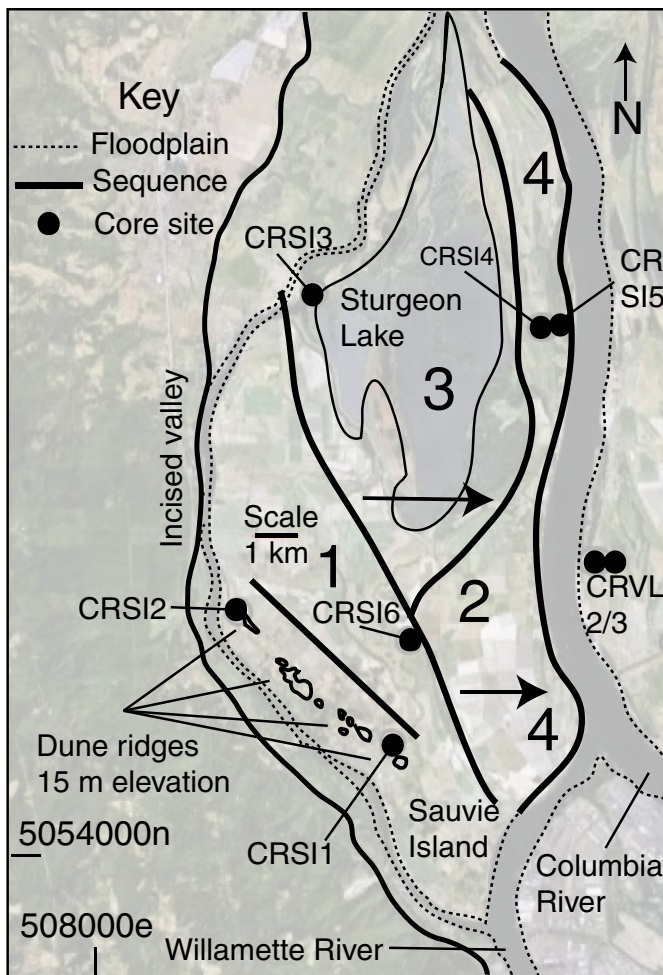


Fig. 11. Map of Sauvie Island floodplain including eolian dune ridges (15-m elevation contour) in the southwest end of the island and the large Sturgeon Lake in the north-center of the floodplain. Floodplain-forming sequences are numbered from 1 oldest to 4 youngest and are based on scroll bar ridges and basal radiocarbon and tephrochronology dates from core sites (Fig. 5). See text for explanation of numbered sequence.

the LCRV. These narrowest reaches of the incised valley (~1.5 km width), which occur upriver of Sand Island (Fig. 2A), generally prohibit the preservation of any sand-shoal islands or contiguous floodplains within the antecedent valley.

Several elongate islands (2.0–4.8 km in length) are present in the lower reaches of the study area where (i) the incised valley is constrained to 2.5–4.5 km width in the antecedent Kalama narrows and (ii) in the lowest study area reaches at Longview where the main channel(s) of the Columbia River are diverted to the opposite side of the incised river valley by the Cowlitz River delta (Fig. 2C). Several small mid-channel islands, including Cottonwood, Lord and Crims Islands, are associated with major bends of then narrow incised valley.

The large and small elongate islands occur in the narrow reaches of the incised river valley, which differ greatly in tidal range between the Washougal and Kalama narrows reaches. The tidal range is about 0.5 m the Reed Island site in the Washougal reach (Fig. 2A) and about 2.1 m at the Longview, WA, in the Kalama narrows reach (Fig. 2C). The elongate islands do not occur in the wider reaches of the Portland basin (Fig. 2B), which has a tidal range of about 1.5 m. These relations demonstrate that elongate island formation is not controlled by tidal range but rather by small incised valley width and the corresponding low sinuosity of major channels in those narrow reaches of the antecedent river valley.

5.6. High sand ridges at major bends in the incised valley

A set of anomalous high ridges (10–20 m in elevation) occurs at the southwest end of Sauvie Island between core sites CRSI1 and CRSI2, along a distance of about 4 km (Fig. 11). The late Holocene ridges are characterized by homogeneous well-sorted fine sand, capped by silt deposits. Both the well-sorted fine sand and capping loess silt at 12–14 m elevations occur well above the maximum height of early-historic (pre-dam) floods of 10.6 m elevation in the Portland Basin (Gates, 1994). Recent eolian dunes of similar heights are evident at Sand Island in the uppermost reaches of the LCRV (Fig. 2A).

The Sauvie Island and Sand Island dune ridges are developed at substantial bends in the south side of the incised river valley (Fig. 2A and B). Temporary stability of main channel bends at these positions permitted sand bars to supply fine sand to the eolian dune ridges during low river level exposures of the shallow channel banks. Channel migrations away from or toward the island, respectively, would either abandon or erode the island dune ridges. Strong bidirectional winds are common in the LCRV, as a result of seasonally reversing pressure gradients between coastal waters and interior basins. Silt topsoils, which cap the eolian dune ridges (Fig. 5), represent loess deposits. The loess silt was remobilized from the LCRV floodplains by strong winds following falling river levels after seasonal floods. The Sauvie Island loess deposits are similar in origin to Holocene loess deposits that mantle late Pleistocene Missoula Flood terraces on the north side of the I–5 CRC traverse (Fig. 2B) (Peterson et al., 2011).

5.7. Large bullseye lakes

Interior flood basin ‘depressions’ formed in the broader floodplains of the Portland basin (Figs. 11 and 12). The ellipsoidal or circular basin depressions were formed by specific sequences of bifurcations or avulsions of sinuosity channels. Channel lateral migration and corresponding point bar accretion produced convex scroll bar ridges in one direction. Following channel avulsion and reversed channel migration the oppositely trending point bar accretion produced an opposing sequence of convex scroll bar ridges. The sequences of opposing channel migrations resulted in bilateral convex scroll bar ridges that surround isolated central depressions. As explained below, the isolated basins were submerged by rising sea level to form the unusual bullseye shaped lakes, as first defined here, including Sturgeon, Vancouver, Shillapoo, and Smith–Bybee Lakes (Fig. 2B). The two largest bullseye lakes in the Portland Basin are Sturgeon Lake (22 km² in area) and Vancouver Lake (11 km²).

We outline the sequences of dated events that produced the Sturgeon and Vancouver Lakes as follows: (i) Major channels migrated toward the incised valley sides of the floodplains prior to about 4 ka (Figs. 11 and 12). (ii) Major channels then avulsed towards the center of the incised valley, thereby isolating floodplain interiors. (iii) Rising sea level in the fluvial–tidal system caused rising groundwater levels in the floodplains to submerge the interior depressions or vegetated wetlands. (iv) Continued major channel migration away from the submerged lakes further distanced the lakes from major channel overbank sedimentation.

The upcore transitions from overbank sandy mud deposits or vegetated wetlands to lacustrine sediment in Sturgeon Lake and Vancouver Lake (Figs. 11 and 12), respectively, are dated to at least 3.4 ka in core site CRSI3 and close to 4.0 ka in core site CRVL7 (Figs. 5 and 6; Table 2). The long-term sedimentation rates in Sturgeon Lake and Vancouver Lake, since 3.4 and 4.0 ka, are 1.0 m and 0.8 m ka^{−1}, respectively (Table 4). The smaller Shillapoo Lake (1.5 km²) in the Vancouver floodplain had a mixed history of lake and vegetated wetland conditions, but it demonstrates a similar low sedimentation rate (1.1 m ka^{−1}) since 4.6 ka. The Smith–Bybee Lakes (7 km² combined surface area) in the Vanport floodplain are reported to have formed after 2.8 ka (Hodges, 2000). The nearby Force Pond (Fig. 10) yielded a sedimentation rate of

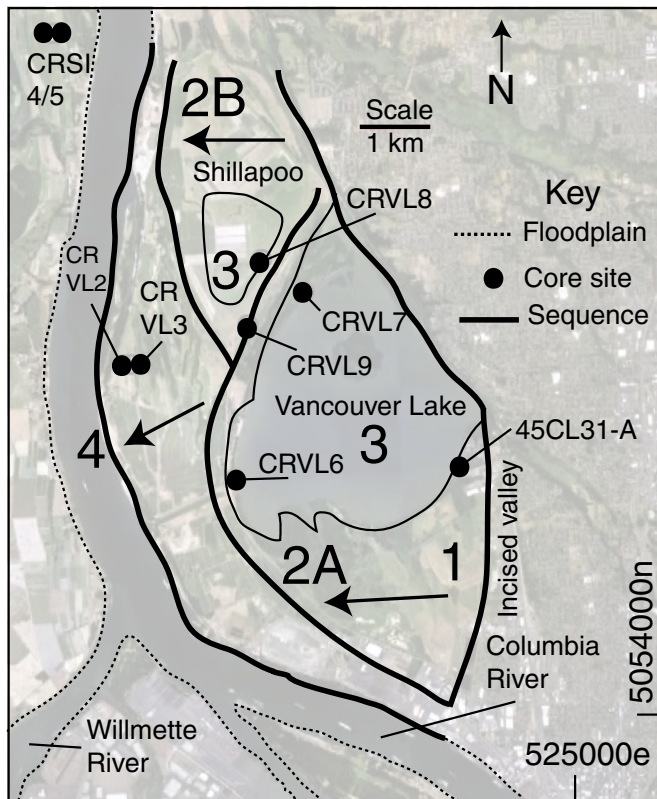


Fig. 12. Map of Vancouver Lake and former Shillapoo Lake in the Vancouver floodplain. Floodplain-forming sequences are numbered from 1 oldest to 4 youngest and are based on scroll bar ridges and basal radiocarbon and tephrochronology dates from core sites (Fig. 6). See text for explanation of numbered sequence. Shillapoo Lake no longer exists and the Vancouver Lake shorelines have receded from the draining of the surrounding floodplains and lowering of seasonal water levels in the Columbia River. Both ongoing impacts lower the groundwater surface in the Vancouver floodplain, which supports water levels in the bullseye lakes. The Vancouver Lake level represents a window into the local groundwater surface in the Vancouver floodplain.

0.6 m ka⁻¹ in site CRXP2 during the last 500 years (Fig. 4; Table 4) when the Columbia River main channel moved to the north side of Hayden Island (Fig. 10).

The bullseye lake sedimentation rates are only slightly lower than the late Holocene rate of sea level rise (~1.25 m ka⁻¹) and the associated rise of the floodplain groundwater surface. Diking and draining of the Sauvie Island floodplain have substantially lowered the floodplain groundwater surface, thereby eliminating many of the smaller lakes and ponds in the floodplains and reducing the depth of Sturgeon Lake (Fig. 13). The long-lived bullseye lakes in the Portland Basin, including Sturgeon, Vancouver, and the Smith–Bybee Lakes are susceptible to decreases in groundwater surface elevation from (i) diking, ditching, and draining of the surrounding floodplains; (ii) groundwater withdrawal from the floodplains; and (iii) seasonal lowering of Columbia River levels by numerous tributary impoundments and deepening of navigation channels in the lower Columbia River (Jay et al., 2011). Future maintenance and preservation of the large bullseye lakes, particularly the shallowing Vancouver Lake (Fig. 6), are entirely dependent on restoring floodplain groundwater surface levels and corresponding lake water levels in the threatened lakes. Reconnecting former floodplain wetland habitats (Fig. 13) to the Columbia River channels for juvenile salmonids, foraging fish, and other aquatic species (Simonstad et al., 1990) will require the removal of dikes and flood gates.

5.8. Long-term sedimentation rates

Short-term sedimentation rates are dependent on proximity to major channels, but long-term sedimentation rates in the Portland

basin have been related to rates of Holocene sea level rise (Peterson et al., 2011). Selected core sites from the Vanport floodplain, including SC8, BH3, BH4, BH7c, and GH8d (Fig. 10), are used to examine the longer-term response of the fluvial–tidal floodplains to slowing rates of sea level rise between middle and latest Holocene time. Average sedimentation rates from core sites BH3, BH4, BH7c and BH8d are estimated for the following age intervals based on tephrochronology and radiocarbon dating: Interval 0–1.3 ka (1.2 m ka⁻¹), interval 1.3–4.0 ka (2.4 m ka⁻¹), interval 4.0–7.7 ka (3.2 m ka⁻¹), and interval 7.7–8.8 ka (8.1 m ka⁻¹) (Table 4). The long-term declines in average sedimentation rates in the Vanport floodplain (Fig. 14) are consistent with declining rates of relative sea level rise in the LCRV between middle and latest Holocene time (Peterson et al., 2011, 2012a). Over time intervals of several thousand years, floodplain surfaces in the LCRV are buried from net submergence under conditions of relative sea level rise. Floodplain burial under conditions of late Holocene net submergence (1.5–3.0 m ka⁻¹) has placed many older floodplain surfaces >3.5 m ka along with any potential archaeological sites, below standard archaeology testing depths (3–5 m subsurface) (Minor et al., 2010).

5.9. Lateral channel migration rates

Permanent loss of the floodplain deposits in the upper reaches of the LCRV occurs from channel migration and associated channel cut-and-fill (Peterson et al., 2012a). Major channel migration rates have been estimated for the larger floodplains in the study area (Figs. 10, 11, and 12). Dated basal deposits in core sites and/or modern channel

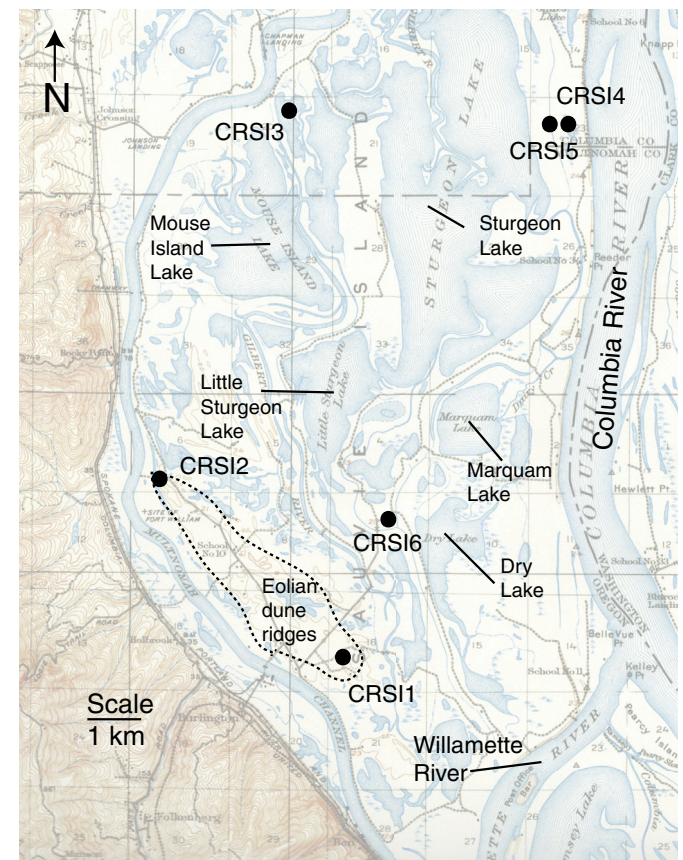


Fig. 13. Partial section of a historic map (1915) of Sauvie Island (USGS, 1915) and an overprint of core sites (solid circles). Diking, ditching, and draining have lowered the floodplain groundwater surface, thereby reducing water depths in Sturgeon Lake (Fig. 5) and eliminating Mouse, Little Sturgeon, and Marquam Lakes, among others. Ongoing lowering of seasonal Columbia River water levels (Jay et al., 2011) threatens the remnant Sturgeon Lake and seasonal wetlands in Sauvie Island.

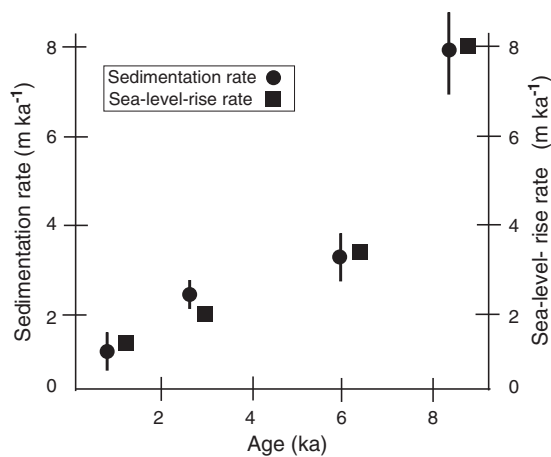


Fig. 14. Plot of averaged sedimentation rates (solid circles with ± 1 Std Dev. bars) versus deposit age intervals in late and middle Holocene deposits from the Vanport floodplain (Fig. 10). We use the onset of tephra eruptions at 1.3 ka (SH/A1.3 ka), 4.0 ka (MSH set-Y), and 7.7 ka (Mazama set-O) (Peterson et al., 2012b) and radiocarbon dates (Table 2) to establish average sedimentation rates in four time intervals in four core sites (BH3, BH4, BH7c, and BH8d) (Table 4). Corresponding rates of relative sea level rise (solid squares) in the LCRV region are from Peterson et al. (2010).

banks (Table 2) are used to estimate channel migration durations (ka) over across-valley separation distances (km) to yield migration rates (km ka^{-1}) (Table 5).

Channel migration rates between dated core site CRSI6 and the modern main channel bank at Sauvie Island (Fig. 11) and between CRVL9 and the modern main channel bank at the Vancouver floodplain (Fig. 12) are 0.9 and 0.7 km ka^{-1} , respectively (Table 5). Alternatively, channel migration rates based on time and distance separations between dated lake deposits at CRSI3 (Sturgeon Lake) and CRVL7 (Vancouver Lake) and core sites at recent shorelines (CRSI4 and CRVL2) are 1.4 and 0.9 km ka^{-1} , respectively. The channel migration from the south side of the Rainier floodplain (CRRF1 at 4.0 ka) to the modern channel bank (1.4 km separation distance) provides the slowest measured rate of 0.35 km ka^{-1} (Figs. 2C and 8). The channel migration or avulsion from the north side of the Vanport floodplain (BH2) to the north side of Hayden Island between BH1 and RC7 (1.5 km separation distance) (Figs. 4 and 10) occurred between 1.3 and 0.5 ka, resulting in the fastest measured migration rate of 1.9 km ka^{-1} (Table 5).

The average lateral migration rate of these across-valley major channel displacements, as presented above, is 1.0 km ka^{-1} or 5 km in the last 5 ka. Using the average channel migration rate and average floodplain width of about 7 km in the Portland basin (Fig. 2B; Table 3) we estimate that 50–75% of the broader floodplains were eroded by major channel migrations in late Holocene time (0–5 ka). Lower preservation potentials are expected for the narrower incised valley widths in the uppermost sections of the Washougal reach (Fig. 2A). The average

Table 5
Late Holocene major channel migration rates.

From/age (ka)	To/age (ka)	Separation distance (km)	Migration rate (km ka^{-1})
CRSI6 (~3.0)	Modern channel	2.7	0.9
CRVL9 (2.8)	Modern channel	2.0	0.7
CRSI3 (~4.0)	CRSI4 (0.5)	4.9	1.4
CRVL7 (~4.0)	CRVL2 (0.5)	3.0	0.9
CRRF1 (4.0)	Modern channel	1.4	0.3
BH2 (1.3)	N.H.Is BH1 (0.5)	1.5	1.9

Notes: Core site and modern channel bank positions are shown in Figs. 10, 11, and 12). Separation distances (km) are based on approximate across-valley (channel perpendicular) orientations.

age of dated overbank deposits that overlie late Holocene channel bank sand (0–5 ka) in all core sites in the study area is 2.5 ka (Table 2), confirming the modest preservation potential of the late Holocene floodplains in the narrow upper reaches of LCRV.

5.10. Local incised valley geometries controlling floodplain preservation

Although incised valley width plays a major role in floodplain preservation potential in the upper reaches of the LCRV some other features of the incised valley also influenced local preservation potential. Major bends in the incised valley stabilized Columbia River channels and associated sand banks that supplied sand to eolian dune ridge development (15–20 m elevation NAVD88) at Sauvie Island and Sand Island (Figs. 2A and B). Dune and loess deposits likely occur in other floodplains in the upper reaches of the LCRV, but their lower elevations (<10 m NAVD88) make their eolian origins difficult to differentiate from river flood deposits.

Major bends in the narrow antecedent valley reaches also diverted major channel thalwegs, allowing mid-channel sand shoals to develop into small elongate islands, such as (i) Reed Island (Fig. 2A) in the narrow Washougal reach and (ii) Cottonwood and Crims Islands in the Kalama narrows (Fig. 3C). Lateral tributary deltas also deflected major channel alignments at confluences of the Cowlitz, Lewis, and Sandy Rivers. These local geomorphic influences are superimposed on system wide conditions of high sediment supply, net sea level rise, and channel lateral migration rates that controlled floodplain development and overbank deposit preservation in the upper reaches of the LCRV.

6. Conclusions

The thicknesses of late Holocene overbank deposits in the upper reaches of the LCRV are generally proportional to the ages of the floodplains. Long-term vertical accretion rates are controlled by submergence and burial under conditions of net sea level rise. However, short-term sedimentation rates are controlled by proximity to major channels and their associated overbank sediment supply. In floodplain sites closest to major channels, the older late Holocene floodplain surfaces (at least 3 ka in age) are buried at depths >3.0 m subsurface, making these sites inaccessible to hand probing techniques. In the most isolated flood basin depressions in the upper reaches of the LCRV, the rate of sea level rise outpaced sedimentation rates, leading to net submergence and the formation of long-lived bullseye lakes.

The adjustments of coastal alluvial systems to sea level rise are generally modeled in terms of river gradient, base level, or base profile. These parameters are all defined by longitudinal profiles. An additional control on floodplain morphology in the upper reaches of the LCRV is the variable width of the incised valley. Specifically, floodplain surface area, channel migration distance, and preservation potential increase with greater incised valley widths. Sedimentation rates and floodplain surface elevations decrease in the wider valley reaches.

The preservation potential of floodplain surfaces in the upper reaches of the LCRV is largely controlled by channel lateral migration rates relative to incised valley widths. However, other features of the incised valley, such as major bends in the antecedent reaches and lateral tributary deltas or tributary mouth shoals, also stabilized major channels on opposite sides of the river valley, permitting the development of some mid-channel islands and eolian dune ridges.

The upper reaches of the LCRV provide examples of late Holocene floodplain development under combined conditions of seasonal river flooding, net sea level rise, and narrow incised-valley constraints. These study results should have relevance to the uppermost reaches of other forearc fluvial–tidal systems around the world.

Supplementary data to this article can be found online at <http://dx.doi.org/10.1016/j.geomorph.2013.07.033>.

Acknowledgments

Coring and surveying assistance in the field was provided by Candice Armijo, Charles Davidshofer, Thomas Eslinger, Corey Friedman, Sean Gallagher, Ashley Gardner, Matthew Gibson, Tracy Handrich, Emily Jenkins, Paulina Kho, Adam Large, Nicholas Misak, Jade Osilla, Jacob Paetsch, Molly Pontifex, Shawn Priddle, Erik Shafer, Harold Shield, Brian Slaughter, Eric Stata, and Justin Sunnarborg. We thank Alan Stewart for providing access to coring sites in Vancouver Lake. Cameron Smith arranged for coring access to the Bachelor Island floodplain. Support for field logistics and core sample radiocarbon dating was provided by Lethbridge College, Lethbridge, Alberta, Canada. Support for the radiocarbon dating of borehole samples in the I-5 CRC traverse was provided by the Columbia River Crossing Project, Washington State Department of Transportation and Oregon Department of Transportation.

References

- Allen, G.P., Posamentier, H.W., 1993. Sequence stratigraphy and facies model of an incised valley fill: the Gironde estuary, France. *Journal of Sedimentary Petrology* 63, 378–391.
- Baker, D., Peterson, C., Hemphill-Haley, E., Twichell, D., 2010. Holocene sedimentation in the Columbia River estuary. *Marine Geology* 273, 83–95.
- Blum, M.D., Törnqvist, T.E., 2000. Fluvial response to climate and sea-level change: a review and look forward. *Sedimentology* 47, 2–48.
- Butler, V.L., 2004. Where have all the native fish gone? The fate of fish that Lewis and Clark encountered on the lower Columbia River. *Oregon Historical Quarterly* 105 (3), 438–463.
- Dalrymple, R.W., Boyd, R., Zaitlin, B.A., 1994. Incised-valley systems: origins and sedimentary sequences. Special Publication No. 51. SEPM Society for Sedimentary Geology, Tulsa, OK, USA.
- Darby, M.C., 1996. Wapato for the People: An Ecological Approach to Understanding the Native American use of *Sagittaria Latifolia* on the Lower Columbia River. (M.A. Thesis) Portland State University, Portland, OR.
- Gates, E.B., 1994. The Holocene Sedimentary Framework of the Lower Columbia River Basin. (M.S. Thesis) Portland State University, Portland, OR.
- Hodges, C., 2000. Geoarchaeological Investigations at 35MU117, Bybee Lake, Wapato Corrections Facility, Multnomah County, Oregon. Edaphos Research, Portland, OR (26 pp.).
- Jay, D.A., Leffler, K., Degens, S., 2011. Long-term evolution of Columbia River tides. *Journal of Waterway, Port, Coastal, and Ocean Engineering*. ASCE 137, 182–191.
- Minor, R., Musil, R.R., Toepel, K.A., 1994. An inventory and assessment of archaeological resources in the Columbia South Shore for the City of Portland, Oregon. Heritage Research Associates Report No. 165. Heritage Research Associates, Eugene, Oregon, USA.
- Minor, R., Peterson, C.D., Carlisle, K.R., 2010. Interstate 5 Columbia River crossing section 106 archaeology technical report. Appendix 1B. Archaeological discovery and evaluation: ODOT parcels. Heritage Research Associates Report No. 344. Heritage Research Associates, Eugene, Oregon, USA.
- Nanson, G.C., Croke, J.C., 1992. A genetic classification of floodplains. *Geomorphology* 4, 459–486.
- O'Rourke, L.M., 2005. The Wapato Valley Predictive Model: Prehistoric Archaeological Site Location on the Floodplain of the Columbia River in the Portland Basin. (M.A. Thesis) Portland State University, Portland, OR.
- Peterson, C.D., Vanderburgh, S., Roberts, M.C., Jol, H.M., Phipps, J.P., Twichell, D.C., 2010. Composition, age, and depositional rates of Holocene shoreface deposits under barriers and beach plains of the Columbia River littoral cell, USA. *Marine Geology* 273, 62–82.
- Peterson, C.D., Minor, R., Peterson, G.L., Gates, E.B., 2011. Pre- and post-Missoula flood geomorphology of the ancestral Columbia River Valley in the Portland forearc basin, Oregon and Washington, USA. *Geomorphology* 129, 276–293.
- Peterson, C.D., Gates, E.B., Minor, R., Baker, D.L., 2012a. Accommodation space controls on latest Pleistocene and Holocene (16–0 ka) sediment size and bypassing in the lower Columbia River valley: a large fluvial-tidal system in Oregon and Washington, USA. *Journal of Coastal Research*. <http://dx.doi.org/10.2112/JCOASTRES-D-12-00172.1>.
- Peterson, C.D., Minor, R., Gates, E.B., Vanderburgh, S., Carlisle, K., 2012b. Correlation of tephra marker beds in latest Pleistocene and Holocene fill of the submerged lower Columbia River valley, Washington and Oregon, U.S.A. *Journal of Coastal Research* 28, 1362–1380.
- Pettigrew, R.M., 1981. A prehistoric culture sequence in the Portland basin of the lower Columbia Valley. University of Oregon Anthropological Papers No. 22. University of Oregon, Eugene, Oregon, USA.
- PugetSoundLidar, 2013. Columbia River 2005—Lidar Metadata. http://pugetsoundlidar.ess.washington.edu/lidardata/metadata/pslc2005Columbia/columbia05_ascii.html (Accessed February 26, 2013).
- Rapp, E.K., 2005. The Holocene Stratigraphy of the Sandy River Delta, Oregon. (M.S. Thesis) Portland State University, Portland.
- Saleeby, B.M., 1983. Prehistoric Settlement Patterns in the Portland Basin of the Lower Columbia River: Ethnohistoric, Archaeological, and Biogeographic Perspectives. (Ph.D. Thesis) University of Oregon, Eugene, OR.
- Sherwood, C.R., Creager, J.S., 1990. Sedimentary geology of the Columbia River estuary. *Progress in Oceanography* 25, 15–79.
- Sherwood, C.R., Jay, D.A., Harvey, B., Hamilton, P., Simenstad, C.A., 1990. Historical changes in the Columbia River estuary. *Progress in Oceanography* 25, 299–352.
- Simenstad, C.A., Small, L.F., McIntire, C.D., Jay, D.A., Sherwood, C.R., 1990. An introduction to the Columbia River estuary: brief history, prior studies and the role of the CREDDP studies. *Progress in Oceanography* 25, 1–14.
- Twichell, D.C., Cross, V.A., Peterson, C.D., 2010. Partitioning of sediment on the shelf offshore of the Columbia River littoral cell. *Marine Geology* 273, 11–31.
- U.S. Geological Survey (USGS), 1905. Topographic Map, Portland Quadrangle, scale 1:62,500.
- US Geological Survey (USGS), 1915. Topographic Map, Hillsboro Quadrangle, scale 1:62,500.
- Wessen, G., 1983. Archaeological investigations at Vancouver Lake, Washington. Report Project Number 115–07. Western Heritage, Inc., Olympia, WA 99–112.